Vertical ground reaction forces diminish in mice after botulinum toxin injection

Sarah L. Manske [a,b], Steven K. Boyd [a,b], Ronald F. Zernicke [a,b,c,*]

[a] Faculty of Kinesiology, University of Calgary, Calgary, Canada
[b] Schulich School of Engineering, University of Calgary, Calgary, Canada
[c] Departments of Orthopaedic Surgery and Biomedical Engineering, School of Kinesiology, University of Michigan, 1402 Washington Heights, 4170 OBL, Ann Arbor, MI 48109, USA

ARTICLE INFO

ABSTRACT

We examined changes in weight-bearing ability in mice after injection with botulinum toxin type A (BTX) to determine whether BTX can be used to isolate the effects of muscle on bone. As ambulation patterns were previously shown to improve within two weeks post-injection, we hypothesized that BTX injection to the posterior hindlimb would not significantly affect the mouse's ability to bear weight in the affected limb one week post-injection. Female BALB/c mice ($N=13$, 16–17 week old) were injected with either 20 μL of BTX (1 U/100 g) or saline (SAL) in the left posterior hindlimb. Vertical ground reaction forces (GRF), hindlimb muscle cross-sectional area (MCSA), and tibial bone micro-architecture were assessed for 42 d following injection. Peak and average vertical GRF were $11 \pm 1\%$ and $23 \pm 3\%$ lower, respectively, in the BTX-injected hindlimb within 4 d post-injection and remained lower than the SAL-injected hindlimb 14–21 d post-injection ($15 \pm 4\%$ and $10 \pm 2\%$, respectively). Time between forelimb and hindlimb peaks was 30–40% greater in the BTX-injected hindlimb than SAL-injected hindlimb 4–14 d post-injection. Peak vertical GRF recovered earlier following BTX injection than MCSA or bone volume fraction. These results indicate that weight-bearing ability recovered despite persistent muscle atrophy, and that weight-bearing alone was insufficient to maintain bone in the absence of muscle activity. We suggest that the absence of high-frequency signals typically associated with fast-twitch muscle activity may be contributing to the ongoing degradation of bone after BTX injection.

1. Introduction

Bone's physiological exposure to loading stems from a combination of muscle and weight-bearing forces. However, whether muscle forces are primarily responsible for bone architecture and mass is an ongoing debate (Burr, 1997; Judex and Carlson, 2009; Robling, 2009).

Due to challenges associated with isolating the independent effects of weight-bearing and muscle forces, it is difficult to discriminate the influence of each loading modality on bone. In paralysis, both muscle and ground reaction forces are affected. Alternatively, tail suspension isolates the loss of ground reaction forces on bone, without affecting potential muscle activity. Indeed, increased anterior muscle activity during tail suspension can actually lead to bone deposition on the anterior tibial surface (Shaw et al., 1987).

A new and unique means to isolate the effects of muscle on bone in an animal model is based on injection with botulinum toxin type A (BTX) (Warner et al., 2006; Gross et al., 2010; Manske et al., 2010a; Poliachik et al., 2010). BTX is a neurotoxin that blocks acetylcholine release at the neuromuscular junction, which results in a loss of contractile ability in affected muscle fibres. The loss of muscle function can last several weeks (Shaari and Sanders, 1993). If muscle causes changes in bone, we would expect to find temporal associations between muscle and bone, such that any change in muscle should precede a change in bone. However, previous studies were unable to detect a lag between recovery of muscle cross-sectional area and bone parameters following BTX injection (Manske et al., 2010a; Poliachik et al., 2010). These findings suggested that either muscle recovery is not required to initiate bone recovery after disuse, or that muscle function recovers earlier than muscle cross-sectional area following BTX injection, triggering bone recovery.

Previous findings suggested that ground reaction forces may be maintained to some degree in BTX-affected limbs despite loss of muscle function, as normal ambulation patterns began to recover two weeks post-injection (Warner et al., 2006). Longino et al. (2005) found that in rabbits with BTX injected to the quadriceps (35 U/100 g), peak vertical GRFs were up to 50% lower in

* Corresponding author at: Departments of Orthopaedic Surgery and Biomedical Engineering, School of Kinesiology, University of Michigan, 1402 Washington Heights, 4170 OBL, Ann Arbor, MI 48109, USA. Tel.: +1 734 764 5210.
  E-mail addresses: zernicke@umich.edu, rfz@ucalgary.ca, mhlewis@umich.edu (R.F. Zernicke).

BTX-injected rabbits than controls six months post-injection. However, to our knowledge, weight-bearing activity has never been quantified in rodents after BTX injection.

In this study, we examined changes in weight-bearing ability after BTX injection to determine whether BTX can be used to isolate the effects of muscle on bone. We hypothesized that BTX injection to the posterior hindlimb may initially decrease, but would not significantly affect the mouse's ability to bear weight in the affected limb one week post-injection. We also hypothesized that weight-bearing ability would recover earlier in the BTX-injected limb than muscle cross-sectional area and bone volume fraction.

2. Materials and methods

2.1. Animal model and experimental design

Female, 16–18 week old, skeletally mature BALB/cAnNCrl (BALB) mice (Beamer et al., 1996; Buie et al., 2008) were obtained from Charles River Laboratories (Saint-Constant, Quebec, Canada). BTX mice ($n=6$) were injected with 20 μL of BTX type A (BOTOX, Allergan Inc., 1 U/100 g body mass) into the left posterior lower limb musculature (a single injection targeting the gastrocnemius, plantaris, and soleus) following baseline body mass, ground reaction forces, and micro-computed tomography measurements. The remaining mice ($n=7$) served as controls and were injected with 20 μL of saline (SAL) into the left posterior hindlimb musculature. In all animals, the right hindlimb served as an internal control.

All animals were housed in groups and provided standard rodent chow and water *ad libitum*. Following BTX injection, they were provided with food and Napa Nectar (SE Lab Group, Napa, CA) on the cage bottom to ease access to food for one week post-injection. Otherwise, normal cage activity was permitted.

Body mass (grams, g) and ground reaction forces (GRFs) were measured 2 d prior to the injections (−2), as well as 4, 7, 14, 21, 28, and 42 d post-injection (Table 1). In addition, muscle and bone micro-architectural outcomes were monitored at 0, 7, 21 and 42 d post-injection with *in vivo* micro-CT. The endpoint was chosen to coincide with the initiation of recovery of muscle and bone following BTX injection (Manske et al., 2010a). At the end of the protocol, mice were euthanized via cervical dislocation while under anaesthesia. All procedures were approved by the Health Sciences Animal Care Committee at the University of Calgary.

2.2. Ground reaction forces

The vertical component of the GRF was measured in independent limbs as mice travelled along a walkway (42 cm long) constructed with four custom-built force platforms (Fig. 1). The walkway was lined with opaque walls (10 cm tall) to allow a continuous landmark easily seen by the mice, so that they would perceive a relatively safe environment (Lepicard et al., 2006). A tunnel was placed at the end of the walkway, which led back to the cage. Prior to baseline measurements, animals were trained to traverse the walkway without stopping or pausing.

Each platform was 3.8 cm × 3.0 cm ($l \times w$). The force platforms employed load cells with a 200 g full scale capacity with a 3000 Ω thin film strain gauge (S250 Miniature Platform Load Cell, Strain Measurement Devices Inc., Meriden CT). The load cells recorded force in the vertical direction only. The platform was calibrated daily using five known masses, ranging from 5 to 40 g.

The platforms were lined individually with paper for each trial. Prior to each trial, the mouse's paws were dipped in ink (forelimbs blue, hindlimbs black) to record location of paw contacts. As such, load profiles could be assigned to the limbs transmitting them. Trials were discarded if the animal stopped forward motion on the platform. Limb measurements were discarded if a limb struck two platforms or if

Table 1
Timeline of measurements for this study. Baseline measurements for body mass and ground reaction forces were made two days prior to the first micro-CT scan and BTX or saline injection. Through the remainder of the study, the measurements made at '−2' are included at day 0.

Measurements	Days							
	−2	0	4	7	14	21	28	42
BTX of SAL Injection		X						
Force platform	X		X	X	X	X	X	X
Micro-CT		X		X		X		X
Muscle mass								X
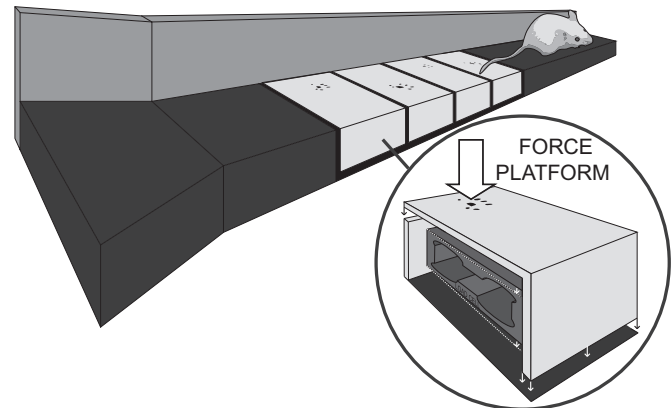
Fig. 1. Walkway with four force platforms used to measure vertical ground reaction forces in mice. For ease of visualization, the right wall is not shown.
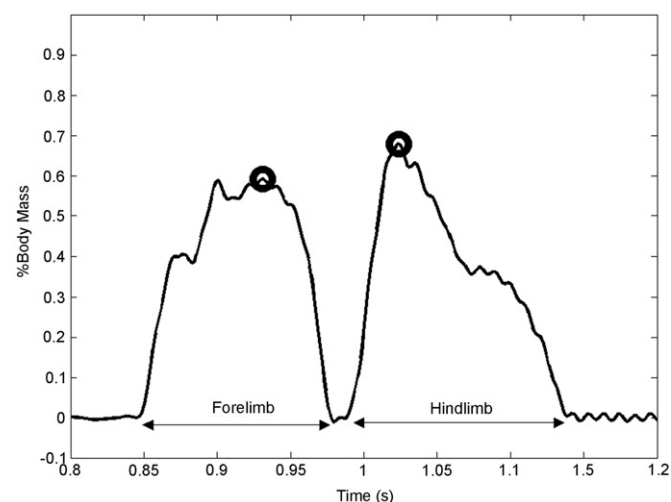
Fig. 2. Typical pattern in the vertical ground reaction force as a function of time on a single platform for the left forelimb (peak on left of image) and left hindlimb (peak on right of image) recorded while the mouse traversed the platform. The circles indicate the peak forelimb and hindlimb forces.

two limbs were on a platform simultaneously. One-to-ten trials were collected per mouse at each time point.

Load cell data were amplified (2310A Signal Conditioning Amplifier, Measurements Group Inc.), and sampled at 1000 Hz (DATAQ Instruments Model DI-205, WinDaq Acquisition DI 720, Akron, OH). Load profiles were filtered with a 60 Hz 2nd-order low-pass Butterworth filter using MATLAB (R2008a, Natick, MA, USA). Peak and average vertical forces were calculated for each limb in each trial (Fig. 2). In addition, time between forelimb and hindlimb peak force, time to peak force, and contact time were assessed as an estimate of speed. For all parameters, the mean value of all trials for each limb on each day is reported. In the few instances where an outcome was missing because of an inadequate trial, the group mean was included for that value.

2.3. In vivo micro-CT

An *in vivo* micro-CT scanner (vivaCT 40, Scanco Medical, Brüttisellen, Switzerland) quantified MCSA and bone outcomes, and scanning procedures were similar to those previously described (Manske et al., 2010a, b). Briefly, mice were anesthetized with isoflurane, and the hindlimbs were positioned and scanned in parallel with a custom fixture (Manske et al., 2010b).

2.4. Muscle outcomes

Muscle cross-sectional area (MCSA, mm^2) was measured in the diaphyseal region of the lower limb. The volume scanned was a 2.65 mm slab encompassing the maximal MCSA. The scanning parameters used were 45 kVP, 133 μA, 620 ms

integration time, 250 projections/180° resulting in a 50 μm isotropic voxel size (Bouxsein et al. 2010).

For each hindlimb a 0.8 mm slab was extracted and Gaussian filtered ($\sigma=1.2$, support=2). All micro-CT image intensities were expressed as a fixed fraction of the maximum gray-scale value (1000). Three threshold values were used to produce segmented images of the entire leg (2.4% of maximal gray-scale value), muscle region excluding the subcutaneous fat (10.6% of maximal gray-scale value), and bone (15% of maximal gray-scale value).

Upon sacrifice, two posterior compartment muscles (gastrocnemius and soleus) as well as tibialis anterior were dissected, and wet muscle masses (mg) were measured.

2.5. Bone outcomes

Each proximal tibial measurement examined a 2.65 mm thick slab, corresponding to 212 slices extending distally from the proximal tibial growth plate. The scanning parameters used were 45 kVP, 133 μA, 200 ms integration time, 2048 samples and 1000 projections/180°, resulting in a 12.5 μm isotropic voxel size.

For each hindlimb, a 1.0 mm volume was extracted from the proximal tibia metaphysis. A semi-automated method was used to separate the trabecular and cortical compartments (Buie et al., 2007). After segmentation, the resulting gray-scale images were Gaussian filtered ($\sigma=1.2$, support=2). A global threshold was applied (30% of maximal gray-scale value) to form binarized images on which morphological analyses were performed.

Bone micro-architecture was assessed with direct 3D methods (Image Processing Language v. 5.07b; Scanco) (Hildebrand and Rüegsegger, 1997). In the trabecular bone region, we examined bone volume (BV) and total volume (TV) as they comprise bone volume fraction (BV/TV, %), as well as trabecular thickness (Tb.Th, mm), trabecular separation (Tb.Sp., mm), trabecular number (Tb.N, mm^{-1}), structural model index (SMI), connectivity density (ConnD, mm^{-3}), and degree of anisotropy (DA).

2.6. Statistical analysis

To assess changes in GRFs, as well as *in vivo* muscle and bone outcomes in each limb, two-way ANOVAs were used with group as a between-subject factor and time as a within-subject factor. *Ex vivo* muscle outcomes were analyzed with a two-way ANOVA, with group as a between-subject factor and limb as a within-subject factor. Analysis of covariance (ANCOVA) was used to determine whether between-group differences were maintained after adjusting for speed (contact time and interpeak time). Simple effects testing with a Bonferroni correction was used to interpret significant interactions. PASW version 17.0 (SPSS Inc., Chicago) was used for all statistical analyses. The significance level was set at $p < 0.05$. Data are presented as mean ± SE.

3. Results

3.1. Force platform outcomes

Qualitatively, we observed changes in paw prints in the BTX-injected hindlimb beginning 4 d post-injection in the BTX group (Fig. 3). These were observed in all of the BTX mice, and lasted 7–21 d post-injection. No changes were noted in other limbs in the BTX mice or in any limbs in the SAL-injected group.

All vertical GRFs were normalized by body mass (%BM, Table 2). Vertical GRFs diminished significantly in the BTX-injected hindlimb post-injection (Fig. 4). Compared with the SAL-injected hindlimb, peak vertical forces were 11 ± 1% lower 4 d post-injection and remained lower (15 ± 4%) 14 d post-injection in the BTX-injected hindlimb (Fig. 4A). Average vertical forces were 23 ± 3% lower 4 d post-injection and remained lower (10 ± 2%) 21 d post-injection. Trends towards lower peak and average forces in the BTX-injected hindlimb persisted until 42 d post-injection. In the right contralateral hindlimb, there were significant group × time interactions for peak and average force; however, the only significant simple effect indicated that average force was greater in the BTX than SAL group at baseline and 4 d post-injection (Fig. 4C). There were no significant main effects or interactions for peak or average forelimb forces on either the left or right sides (Figs. 4B and D).

There was some indication that gait speed changed subtly following BTX-injection as there were significant group × time interactions for contact time and interpeak time on both the left injected side and right contralateral side (Fig. 5). Although there were no significant simple effects for contact time, interpeak time for the left side was 37 ± 5% higher in the BTX than SAL group 4 d post-injection, and remained higher (40 ± 4%) 14 d post-injection. On the right side, interpeak time was 35 ± 3% lower in the BTX than SAL group at baseline. There was also a low, but significant correlation ($r=-0.27$, $p < 0.001$) between interpeak time and
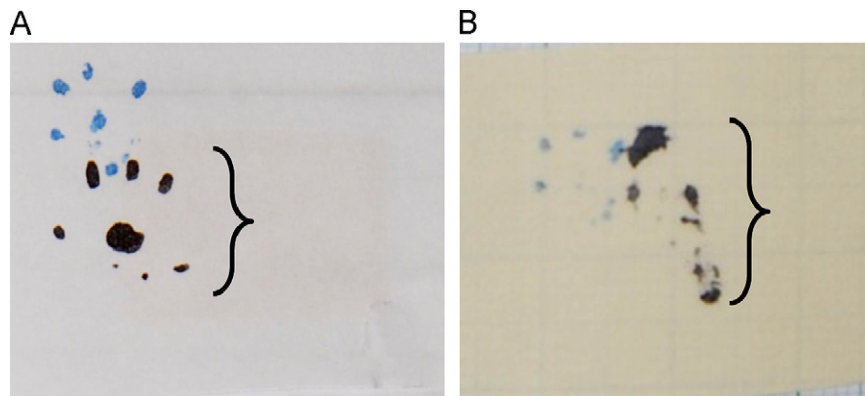

Fig. 3. Typical hindlimb prints (black, with parentheses) recorded at (A) baseline, and (B) 4 d after BTX injection. The lighter (blue) prints indicate the left forelimb prints. Individual digits in the black hindlimb prints are not as easily visualized post-injection, suggesting a different mechanism for weight-bearing.

Table 2
Body mass measured from baseline to 42 d post-injection.

	Days						
	−2	4	7	14	21	28	42
BTX	24.1 ± 0.7	22.4 ± 0.3	22.8 ± 0.5	23.0 ± 0.4	23.6 ± 0.3	23.9 ± 0.4	26.0 ± 0.6
Saline	21.9 ± 0.3	21.8 ± 0.4	21.8 ± 0.4	22.3 ± 0.4	22.4 ± 0.3	22.2 ± 0.5	22.7 ± 0.6

Values are the mean ± SE, $n=6$ for BTX, $n=7$ for saline.
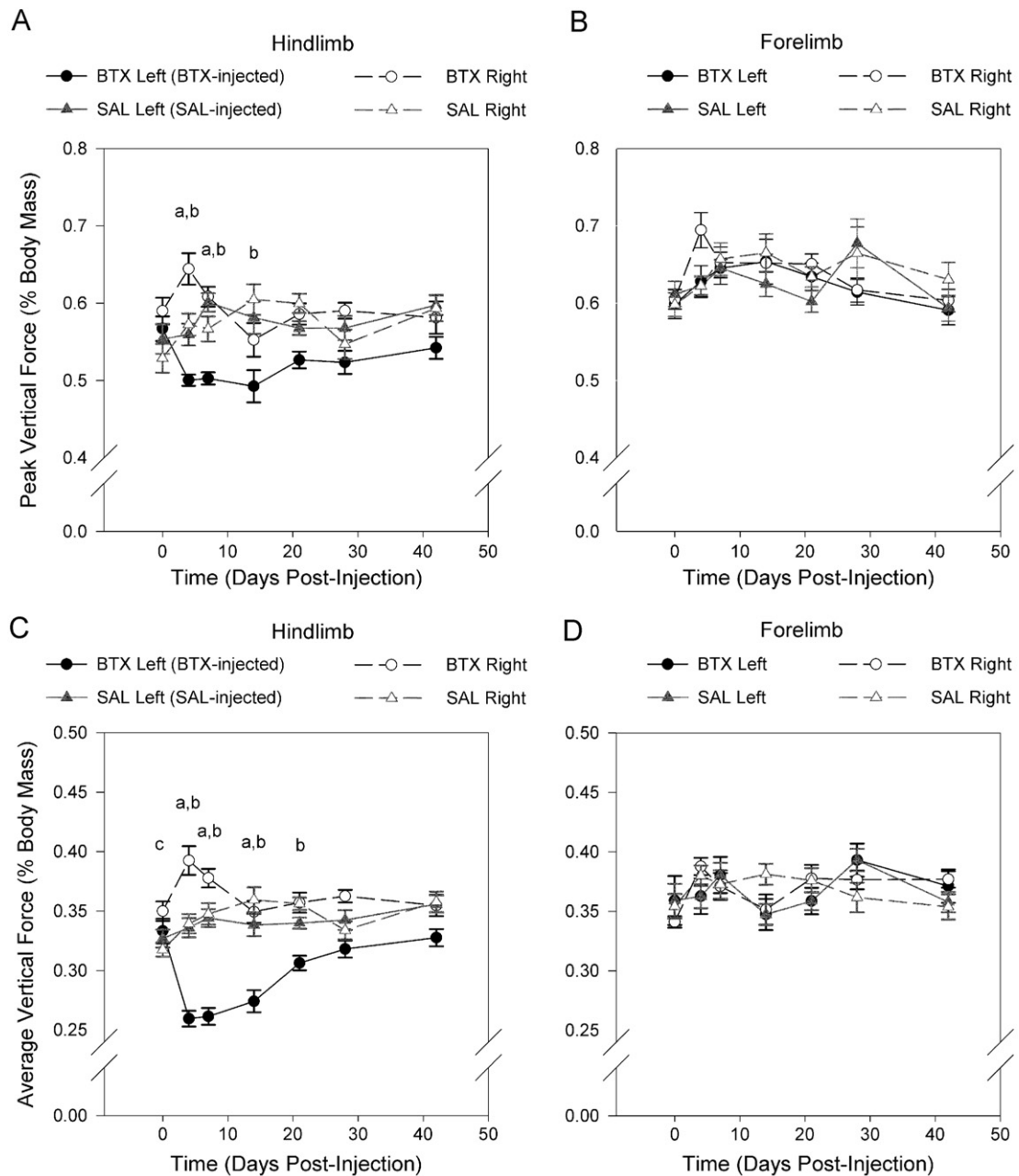
Fig. 4. Peak (A,B) and average (C,D) vertical ground reaction forces measured from baseline to 42 d post-injection in the hindlimb (A,C) and forelimb (B,D). Values are group mean $\pm$ SE. Significant differences ($p < 0.05$) determined by simple effect tests with Bonferroni adjustments are indicated by the following: [a]BTX Left (injected) < BTX Right, [b]BTX Left (injected) < SAL Left (injected), [c]BTX Right > SAL Right.

hindlimb peak force. There were no significant group or interaction effects for time to peak force.

After adjusting for interpeak time, the between-group differences in peak vertical force were no longer significant in the injected hindlimb (data not shown). However, after adjusting for interpeak time, the between-group differences in average hindlimb vertical force remained significant for 4, 7, 14, and 21 d post-injection. Similarly, after adjusting for contact time, between-group differences in peak or average vertical force remained significant.

3.2. Muscle Properties

MCSA was significantly lower in the BTX-injected hindlimb than the SAL-injected hindlimb from 7 d ($16 \pm 2\%$) to 42 d ($41 \pm 4\%$)

post-injection. MCSA was also lower than baseline values in the BTX-injected hindlimb. Further, gastrocnemius, soleus, and tibialis anterior mass were significantly lower in the BTX-injected hindlimb than the SAL-injected hindlimb ($37 \pm 8\%$, $22 \pm 9\%$, $67 \pm 4\%$, respectively) at day 42. In the right contralateral hindlimbs, MCSA was $8 \pm 2\%$ lower in the BTX than SAL group from day 21 to day 42.

3.3. Bone properties

Bone micro-architectural properties declined significantly post-injection. Specifically, in the BTX-injected hindlimb when compared with baseline, BV/TV was $19 \pm 10\%$ lower beginning 21 d post-injection, and this decrease was maintained until 42 d post-injection ($28 \pm 14\%$). ConnD, Tb.N, and Tb.Sp showed similar patterns of degradation in the BTX-injected hindlimb only (data
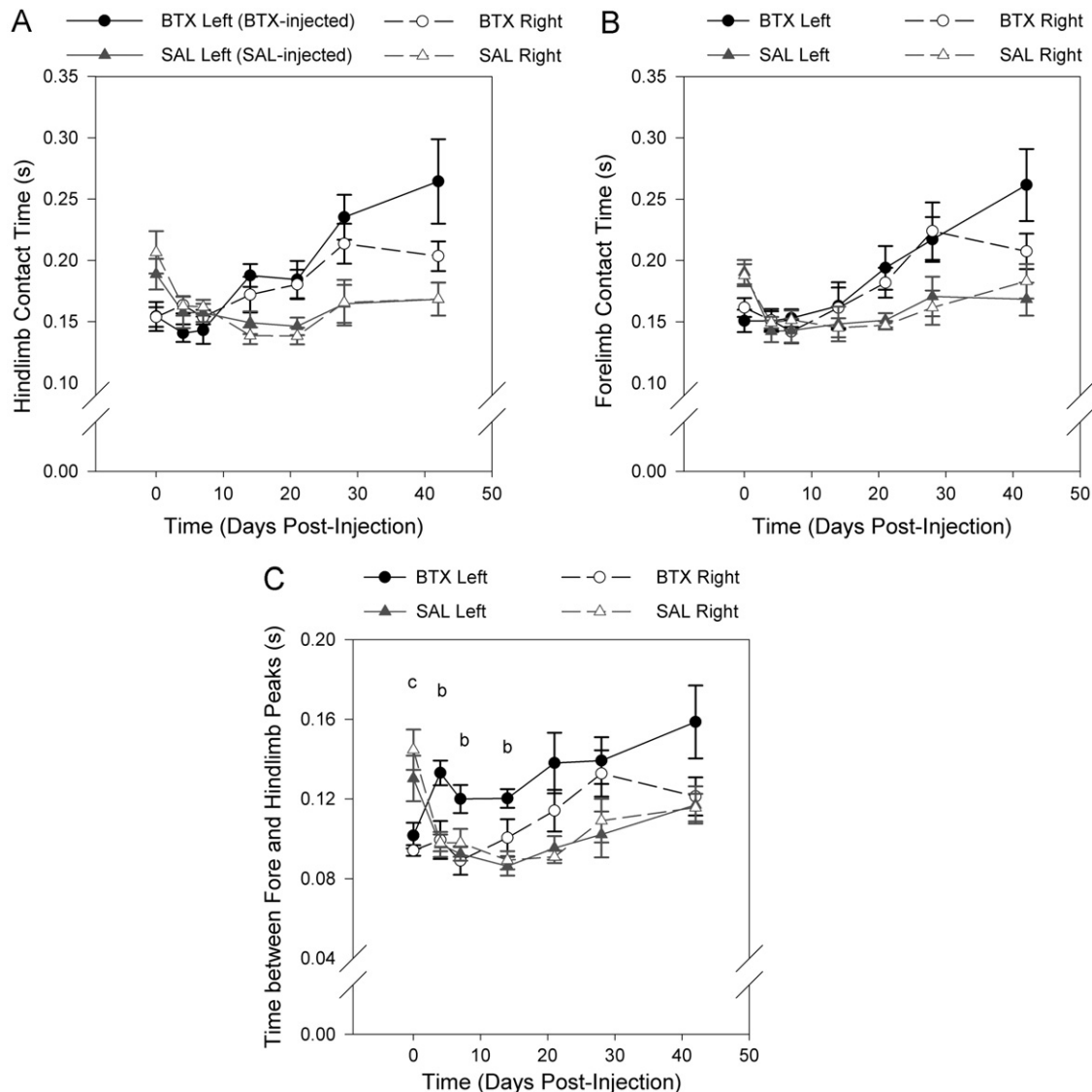
Fig. 5. Contact times for hindlimb (A) and forelimb (B), and time between forelimb and hindlimb peak vertical ground reaction forces (C) measured from baseline to 42 d post-injection. Values are group mean $\pm$ SE. Significant differences ($p < 0.05$) determined by simple effect tests with Bonferroni adjustments are indicated by the following: [b]BTX Left (injected) < SAL Left (injected), [c]BTX Right > SAL Right.

not shown). There was also a significant group × time interaction for Tb.Th; however, no simple effects were significant. There were no significant main effects or interactions for DA or SMI.

3.4. Relative changes

In the BTX-injected hindlimb, peak vertical GRFs appeared to recover earlier than MCSA and BV/TV as peak vertical GRF were no different than the baseline values within 14 d post-injection (Fig. 6). In contrast, MCSA and BV/TV remained lower than baseline in the BTX-injected hindlimb than SAL-injected hindlimb 42 d post-injection. Further, despite persistently lower MCSA, average and peak vertical GRFs recovered to normal values prior to the end of the experiment.

4. Discussion

In this study, we found that weight-bearing ability, assessed by peak and average vertical forces, was diminished in the murine BTX-injected hindlimb for 14–21 d post-injection. In addition, we demonstrated that weight-bearing ability began to recover despite increase in muscle atrophy 21 d post-injection. Since BV/TV continued to decline with MCSA, these findings indicate that weight-bearing alone was insufficient to maintain bone in the absence of muscle activity. This research suggests that the absence of normal mechanical signals from the affected muscles may have led to the continued deterioration of bone.

There are several possible explanations related to muscle properties that may have contributed to the earlier recovery of vertical GRFs than MCSA. First, compensation by unaffected muscle groups (e.g., quadriceps) may have allowed normal ambulation despite functional deficits in other muscles (Misiaszek and Pearson, 2002). Second, compensation by unaffected muscle fibres within the injected muscles may also have contributed to recovery. The gait patterns studied likely did not require full activation of all posterior muscle fibres. Some motor units may have been unaffected by BTX, although near complete inhibition should have occurred at the dose used in this study (Stone et al., 2007). In addition, slow-twitch muscle fibres, primarily used for postural
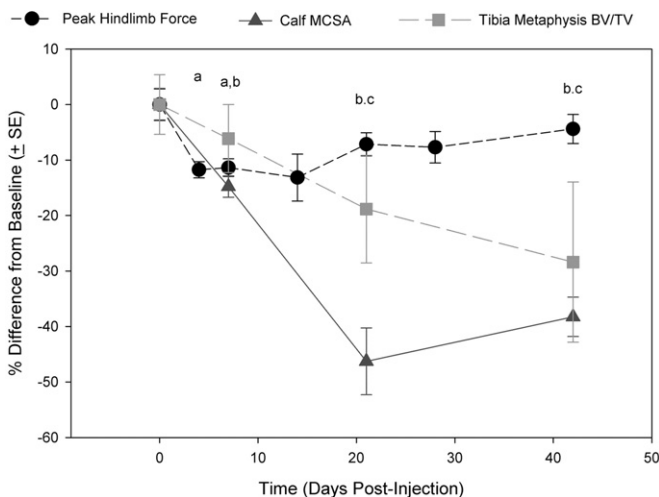
Fig. 6. Peak vertical ground reaction force (GRF), muscle cross-sectional area (MCSA), and proximal tibia metaphyseal bone volume fraction (BV/TV) in the BTX-injected limb plotted against time post-injection, expressed as a percentage of the baseline value. At each time point, significant differences ($p < 0.05$) from baseline determined by simple effect tests with Bonferroni adjustments are indicated for the following variables: [a]peak hindlimb force, [b]MCSA, and [c]BV/TV.

muscle activity, have been shown to recover earlier than fast-twitch fibres following BTX injection (Duchen, 1970). Third, Schmitt et al. (2010) demonstrated that muscle mass was not directly linked with GRFs as they found no difference in peak vertical forces during walking between hypermuscular and wild-type mice. Finally, muscle function may recover earlier than muscle mass following BTX injection (Ma et al., 2004; Keller, 2006), which indicates that muscle contractile function may explain the earlier recovery in GRFs.

In addition, the nervous system may play a role in the recovery of weight-bearing. Bain et al. (2010) found that animals lacking proprioceptive feedback experienced a lesser degree of bone loss following BTX injection. This result suggested that bone loss due to a loss of muscle activity is mediated by the nervous system. In addition, Sample et al. (2008, 2010) found that unilateral loading triggered an osteogenic response in the contralateral side that was mitigated when neural signals were blocked. These combined results indicate that the nervous system may play a key role in the interaction between muscle and bone.

The peak vertical forces measured at baseline in the present study ($\sim$56% BM for hindlimb; $\sim$61% BM for forelimb) were similar to those previously reported ($\sim$58% BM for hindlimb; $\sim$64% BM for forelimb) (Clarke et al., 2001). These findings suggest that peak vertical GRFs, as well as relative forelimb and hindlimb load-sharing, are relatively similar across different strains and ages of mice. We also demonstrated that between-group differences in gait could be detected using vertical GRFs despite relatively large within-subject variability.

Measuring murine GRFs is challenging, and our force platform was designed to measure only the vertical component of the ground reaction force as this component supports the animal's weight (Biewener, 2003). A tri-axial load cell would have permitted transverse force measurements; however, at maximum, antero-posterior and mediolateral forces reach approximately 10% BM in the mouse (Zumwalt et al., 2006). Thus any difference in these forces, which could reflect changes in the mouse's balance (Biewener, 2003), were likely to be small and unreliable (Howard et al., 2000). Further, we used foot contact time and interpeak time as surrogate measures of velocity (Bertram et al., 2000). As interpeak time could account for between-group differences in peak hindlimb vertical force, it is possible that lower peak vertical forces were a result of slower

movement in the BTX-affected limb. Regardless of whether changes in weight-bearing were due to changes in gait speed, our data unequivocally suggest that weight-bearing, and thus the strains experienced by the bone, diminished in the BTX-affected limb. Further, Rubin and Lanyon (1982) showed using in vivo strain gauge measurements in dogs and horses that bone strain rate increases linearly with gait speed. Therefore, we would expect that the bone's strain environment would be significantly altered with a change in gait speed.

To our knowledge, this is the first study to longitudinally examine GRFs in mice in conjunction with muscle and bone outcomes. In our previous longitudinal study, corroborated by Poliachik et al. (2010), we found that maximum muscle and bone atrophy occurred 28 d post-injection, and subsequently began to recover (Manske et al., 2010a). This suggested that there was no delay between muscle and bone recovery following BTX injection. The findings from the present study lend further support to the synchronicity between MCSA and BV/TV, and add to this by demonstrating that weight-bearing ability began to recover earlier than MCSA and BV/TV. We used BV/TV to represent bone microarchitecture as it encompasses many properties of the bone microarchitecture and is highly sensitive to change. However, even after combining the results of these studies, it is difficult to ascertain whether weight-bearing ability could be the trigger for bone recovery that we previously observed between 28 and 56 d post-injection (Manske et al., 2010a).

The implications of these findings on our understanding of the interaction between muscle and bone are further confounded by the difference in recovery from BTX, microgravity, and hindlimb unloading. During reambulation after hindlimb unloading and microgravity, return of weight-bearing is rapidly followed by a recovery of muscle volume (Akima et al., 2000; Allen et al., 2006), but a delayed recovery of bone (Allen et al., 2006; Sibonga et al., 2007). We would also expect to observe a lag in bone recovery because of the relatively longer bone formation period than resorption period, and the delay between new bone formation and the complete mineralization of that new bone (Eriksen et al. 1984a, 1984b; Jee, 2001). Thus, bone recovery likely begins earlier than can be detected with micro-CT.

In conclusion, we found that BTX did not purely isolate the effects of muscle force on bone as GRFs diminished temporarily post-injection. However, our finding that GRFs recover earlier than BV/TV suggests that although the mouse was able to compensate to maintain normal gait, bone homeostasis could not be maintained by weight-bearing alone. We suggest that the absence of high-frequency signals typically associated with fast-twitch muscle activity may be contributing to the ongoing degradation of bone (Huang et al., 1999). More detailed analyses of both muscle force production and the bone strain environment are required to fully understand how muscle forces affect bone adaptation. Nevertheless, evidence from this study suggests that both weight-bearing and muscle forces are likely required to maintain bone integrity.

Conflict of interest statement

All authors have no conflict of interest to disclose.

Acknowledgements

References

Akima, H., Kawakami, Y., Kubo, K., Sekiguchi, C., Ohshima, H., Miyamoto, A., Fukunaga, T., 2000. Effect of short-duration spaceflight on thigh and leg muscle volume. Med. Sci. Sports Exerc. 32, 1743–1747.

Allen, M.R., Hogan, H.A., Bloomfield, S.A., 2006. Differential bone and muscle recovery following hindlimb unloading in skeletally mature male rats. J. Musculoskelet. Neuronal Interact. 6, 217–225.

Bain, S., Poliachik, S., Threet, D., Srinivasan, S., Gross, T.S., 2010. Trabecular bone homeostasis is modulated by neuromuscular proprioception. J. Bone Miner. Res. 25 (Suppl. 1) SU0106 Available at < http://www.asbmr.org/Itinerary/Detail.aspx?id=b5104288-b37d-4cf3-9c86-213e487a94ab > . Accessed on October 19, 2010.

Beamer, W.G., Donahue, L.R., Rosen, C.J., Baylink, D.J., 1996. Genetic variability in adult bone density among inbred strains of mice. Bone 18, 397–403.

Bertram, J.E., Lee, D.V., Case, H.N., Todhunter, R.J., 2000. Comparison of the trotting gaits of labrador retrievers and greyhounds. Am. J. Vet. Res. 61, 832–838.

Biewener, A.A., 2003. Animal Locomotion. Oxford University Press, New York.

Bouxsein, M.L., Boyd, S.K., Christiansen, B.A., Guldberg, R.E., Jepsen, K.J., Müller, R., 2010. Guidelines for assessment of bone microstructure in rodents using micro-computed tomography. J. Bone Miner. Res. 25, 1468–1486.

Buie, H.R., Campbell, G.M., Klinck, R.J., MacNeil, J.A., Boyd, S.K., 2007. Automatic segmentation of cortical and trabecular compartments based on a dual thresh-old technique for in vivo micro-CT bone analysis. Bone 41, 505–515.

Buie, H.R., Moore, C.P., Boyd, S.K., 2008. Postpubertal architectural developmental patterns differ between the L3 vertebra and proximal tibia in three inbred strains of mice. J. Bone Miner. Res. 23, 2048–2059.

Burr, D.B., 1997. Muscle strength, bone mass, and age-related bone loss. J. Bone Miner. Res. 12, 1547–1551.

Clarke, K.A., Smart, L., Still, J., 2001. Ground reaction force and spatiotemporal measurements of the gait of the mouse. Behav. Res. Methods Instrum. Comput. 33, 422–426.

Duchen, L.W., 1970. Changes in motor innervation and cholinesterase localization induced by botulinum toxin in skeletal muscle of the mouse: differences between fast and slow muscles. J. Neurol. Neurosurg. Psychiatry 33, 40–54.

Eriksen, E.F., Gundersen, H.J., Melsen, F., Mosekilde, L., 1984a. Reconstruction of the formative site in iliac trabecular bone in 20 normal individuals employing a kinetic model for matrix and mineral apposition. Metab. Bone Dis. Relat. Res. 5, 243–252.

Eriksen, E.F., Melsen, F., Mosekilde, L., 1984b. Reconstruction of the resorptive site in iliac trabecular bone: a kinetic model for bone resorption in 20 normal individuals. Metab. Bone Dis. Relat. Res. 5, 235–242.

Gross, T.S., Poliachik, S.L., Prasad, J., Bain, S.D., 2010. The effect of muscle dysfunction on bone mass and morphology. J. Musculoskelet. Neuronal Interact. 10, 25–34.

Hildebrand, T., Rüegsegger, P., 1997. A new method for the model-independent assessment of thickness in three-dimensional images. J. Microsc. 185, 67–75.

Howard, C.S., Blakeney, D.C., Medige, J., Moy, O.J., Peimer, C.A., 2000. Functional assessment in the rat by ground reaction forces. J. Biomech. 33, 751–757.

Huang, R.P., Rubin, C.T., McLeod, K.J., 1999. Changes in postural muscle dynamics as a function of age. J. Gerontol. A Biol. Sci. Med. Sci. 54, B352–B357.

Jee, W.S.S., 2001. Integrated bone tissue physiology: anatomy and physiology. In: Cowin, S.C. (Ed.), Bone Mechanics Handbook. CRC Press, Boca Raton 1-1–1-68.

Judex, S., Carlson, K.J., 2009. Is bone's response to mechanical signals dominated by gravitational loading? Med. Sci. Sports Exerc. 41, 2037–2043.

Keller, J.E., 2006. Recovery from botulinum neurotoxin poisoning in vivo. Neuroscience 139, 629–637.

Lepicard, E.M., Venault, P., Abourachid, A., Pelle, E., Chapouthier, G., Gasc, J.P., 2006. Spatio-temporal analysis of locomotion in BALB/cByJ and C57BL/6J mice in different environmental conditions. Behav. Brain Res. 167, 365–372.

Longino, D., Frank, C., Leonard, T.R., Vaz, M.A., Herzog, W., 2005. Proposed model of botulinum toxin-induced muscle weakness in the rabbit. J. Orthop. Res. 23, 1411–1418.

Ma, J., Elsaidi, G.A., Smith, T.L., Walker, F.O., Tan, K.H., Martin, E., Koman, L.A., Smith, B.P., 2004. Time course of recovery of juvenile skeletal muscle after botulinum toxin A injection: an animal model study. Am. J. Phys. Med. Rehabil. 83, 774–780 quiz 781-3.

Manske, S.L., Boyd, S.K., Zernicke, R.F., 2010a. Muscle and bone follow similar temporal patterns of recovery from muscle-induced disuse due to botulinum toxin injection. Bone 46, 24–31.

Manske, S.L., Boyd, S.K., Zernicke, R.F., 2010b. Muscle changes can account for bone loss after botulinum toxin injection. Calcif. Tissue Int. 87 (6), 541–549.

Misiaszek, J.E., Pearson, K.G., 2002. Adaptive changes in locomotor activity following botulinum toxin injection in ankle extensor muscles of cats. J. Neurophysiol. 87, 229–239.

Poliachik, S.L., Bain, S.D., Threet, D., Huber, P., Gross, T.S., 2010. Transient muscle paralysis disrupts bone homeostasis by rapid degradation of bone morphology. Bone 46, 18–23.

Robling, A.G., 2009. Is bone's response to mechanical signals dominated by muscle forces? Med. Sci. Sports Exerc. 41, 2044–2049.

Rubin, C.T., Lanyon, L.E., 1982. Limb mechanics as a function of speed and gait: a study of functional strains in the radius and tibia of horse and dog. J. Exp. Biol. 101, 187–211.

Sample, S.J., Behan, M., Smith, L., Oldenhoff, W.E., Markel, M.D., Kalscheur, V.L., Hao, Z., Miletic, V., Muir, P., 2008. Functional adaptation to loading of a single bone is neuronally regulated and involves multiple bones. J. Bone Miner. Res. 23, 1372–1381.

Sample, S.J., Collins, R.J., Wilson, A.P., Racette, M.A., Behan, M., Markel, M.D., Kalscheur, V.L., Hao, Z., Muir, P., 2010. Systemic effects of ulna loading in male rats during functional adaptation. J. Bone Miner. Res. 25, 2016–2028.

Schmitt, D., Zumwalt, A.C., Hamrick, M.W., 2010. The relationship between bone mechanical properties and ground reaction forces in normal and hypermuscular mice. J. Exp. Zool. A Ecol. Genet. Physiol. 313, 339–351.

Shaari, C.M., Sanders, I., 1993. quantifying how location and dose of botulinum toxin injections affect muscle paralysis. Muscle Nerve 16, 964–969.

Shaw, S.R., Zernicke, R.F., Vailas, A.C., Deluna, D., Thomason, D.B., Baldwin, K.M., 1987. Mechanical, morphological and biochemical adaptations of bone and muscle to hindlimb suspension and exercise. J. Biomech. 20, 225–234.

Sibonga, J.D., Evans, H.J., Sung, H.G., Spector, E.R., Lang, T.F., Oganov, V.S., Bakulin, A.V., Shackelford, L.C., Leblanc, A.D., 2007. Recovery of spaceflight-induced bone loss: bone mineral density after long-duration missions as fitted with an exponential function. Bone 41, 973–978.

Stone, A.V., Ma, J., Whitlock, P.W., Koman, L.A., Smith, T.L., Smith, B.P., Callahan, M.F., 2007. Effects of botox and neuronox on muscle force generation in mice. J. Orthop. Res. 25, 1658–1664.

Warner, S.E., Sanford, D.A., Becker, B.A., Bain, S.D., Srinivasan, S., Gross, T.S., 2006. Botox induced muscle paralysis rapidly degrades bone. Bone 38, 257–264.

Zumwalt, A.C., Hamrick, M., Schmitt, D., 2006. Force plate for measuring the ground reaction forces in small animal locomotion. J. Biomech. 39, 2877–2881.